Stochastic Hydrology and Hydraulics 11: 33-50

Reliability analysis of hydraulic structures considering unit hydrograph uncertainty

B. Zhao
Engineering Division, Flood Control District of Marcipoa County, 2801 W. Durango Street, Phoenix, AZ 85009, USA

Y.-K. Tung
Wyoming Water Resources Center and Statistics Department, University of Wyoming, Laramie, WY 82071, USA

K.-C. Yeh and **J.-C. Yang**
Department of Civil Engineering, National Chiao-Tung University, Hsinchu, Taiwan, ROC

Abstract: Unit hydrographs (UHs), along with design rainfalls, are frequently used to determine the discharge hydrograph for design and evaluation of hydraulic structures. Due to the presence of various uncertainties in its derivation, the resulting UH is inevitably subject to uncertainty. Consequently, the performance of hydraulic structures under the design storm condition is uncertain. This paper integrates the linearly constrained Monte-Carlo simulation with the UH theory and routing techniques to evaluate the reliability of hydraulic structures. The linear constraint is considered because the water volume of each generated design direct runoff hydrograph should be equal to that of the design effective rainfall hyetograph or the water volume of each generated UH must be equal to one inch (or cm) over the watershed. For illustration, the proposed methodology is applied to evaluate the overtopping risk of a hypothetical flood detention reservoir downstream of Tong-Tou watershed in Taiwan.

Keywords: Unit hydrograph, uncertainty analysis, linearly constrained Monte-Carlo simulation, reliability analysis.

1 Introduction

Since Freudenthal (1947, 1956) first pioneered the structural reliability concept in the area of civil engineering, much effort has been devoted to solving load-resistance interaction problems (Ang and Tang, 1984; Shinozuka, 1964; Shinozuka, 1981; Yen et al., 1986). The effort has resulted in many practical solution methods for reliability analysis. The reliability of a hydraulic structure is the probability that the load does not exceed the capacity or the resistance of the hydraulic structure. On the other hand, the risk is the probability that the load exceeds the resistance causing the failure of a hydraulic structure. Failures can be broadly classified into performance failure and structural failure. Herein, the term 'failure' is used in a very general manner. The specific definition of the failure would depend on the problem to be addressed.

Due to the presence of various uncertainties, reliability analysis is becoming an important task in the design and analysis of hydrosystems or hydraulic structures. The methods for hydraulic structures reliability analysis can be classified into direct inte-

gration method, safety margin and safety factor method, first-/second-order methods, dynamic (time-dependent) reliability methods, and Monte-Carlo simulation and its variations (Yen et al., 1986; Mays and Tung, 1992; Yen and Tung, 1993). Monte-Carlo simulation methods implicitly consider the load-resistance interaction whereas the other methods do so explicitly.

As discussed by Shinozuka (1989), Monte-Carlo simulation methods are becoming more promising and practically feasible tools in reliability analysis because (1) many much more complex real-life problems can be solved as computational hardware and software capabilities expand with accelerated speed, and (2) there are many large problems which simply cannot be approximated by explicit methods. In the area of hydraulic structure reliability analysis, hydraulic or hydrologic routing is often required to evaluate the failure probability of a hydraulic structure, which makes the explicit evaluation of the risk difficult, if not impossible. This paper focuses on integrating Monte-Carlo simulation with the unit hydrograph (UH) theory and routing techniques to evaluate the failure probability of a hydraulic structure. The failure probability of a hydraulic structure is computed by the fraction of simulations which produce inflows that cause the occurrences of failure to the hydraulic structure. Due to the mass balance constraint of input and output in a surface watershed system or the unity constraint for a UH, the linearly constrained Monte-Carlo simulation, in particular, will be applied.

The UH theory is one of the most widely used hydrologic engineering tools for rainfall-runoff analysis. It is based on linear and time-invariant system theory, which leads to a convolution relationship among the effective rainfall hyetograph (ERH), direct runoff hydrograph (DRH), and UH. Based on the UH theory, the ERH and DRH are, respectively, the input to and output from a surface watershed; and the UH is the transformation function uniquely characterizing the surface watershed system. Once a UH for the surface watershed is derived from historical storm data, the selected design ERH is convolved with the UH to obtain a design DRH for the purposes of hydraulic structure design and analysis. In a discrete-time and matrix framework, the convolution relationship can be written as (Chow et al., 1988)

$$\mathbf{p}_{\mathrm{dsgn}}\mathbf{u} = \mathbf{q}_{\mathrm{dsgn}} \tag{1}$$

in which $\mathbf{P}_{\mathrm{dsgn}}$ is a special Toeplitz matrix with its columns whose elements made up of shifted-down design ERH ordinates; $\mathbf{u}$ is a column vector of UH ordinates; and $\mathbf{q}_{\mathrm{dsgn}}$ is a column vector containing the design DRH ordinates. In turn, the computed design DRH, $\mathbf{q}_{\mathrm{dsgn}}$, combined with the baseflow, serves as the input to the hydraulic structure located downstream of the surface watershed. Then, the performance of the hydraulic structure can be evaluated by routing the design flow hydrograph through the hydraulic structure such as a detention reservoir, or levee.

Because of measurement and data-processing errors in the ERH and DRH and possible violation of assumptions for the UH theory, the derived UH is always subject to a certain degree of uncertainty. The uncertainties associated with the UH, through the convolution operation as shown in Eq.(1), will be transmitted to the design DRH. Therefore, the UH and DRH are random vectors. If the UH uncertainty features such as the mean vector and covariance matrix are known or quantified from an uncertainty analysis, Eq. (1) then can be used to analytically derive the mean and covariance matrix of the design DRH. With an assumed probability distribution, Monte-Carlo simulation can be used to generate random DRH vectors. Some example

applications of Monte-Carlo simulation can be found in stream flow generation for purpose of reservoir and river system design (Fiering and Jackson, 1971; Hufschmidt and Fiehag, 1966), freeboard design of river bank (Mizumura and Ouazar, 1992), and excavation scheduling in open pit coal mining operation affected by groundwater drawdown (Nguyen and Chowdhury, 1985). When a random vector, without being subject to any constraints, follows a multivariate normal distribution, the generation of random vectors can be performed by several efficient techniques (Ang and Tang, 1984; Borgman, 1990). The generated DRH vectors, combined with the baseflow, are routed through the hydraulic structure located downstream of the surface watershed. It is conceivable that some of the generated DRH vectors may cause the failure of the hydraulic structure. The fraction of simulations in which failure incidents occur is the risk or the failure probability and such information is essential for the evaluation and modification of the hydraulic structure.

By the law of mass conservation, the water volume of each generated DRH must be equal to that of the design ERH or, by definition, the water volume of each generated UH should be equal to one inch (or cm) over the watershed. Such physical constraints should be preserved in the Monte-Carlo simulation which generates random UHs and design DRHs. In particular, the linear constrained Monte-Carlo simulation is applicable to the problem in hand. The linearly constrained MontesCarlo simulation may be conducted by using the acceptance-rejection method which was first proposed by von Neumann (1951). Detail discussions on the acceptance-rejection method are given by Rubinstein (1981). The acceptance-rejection methods depend on a much larger number of simulations in order to satisfy the constraint and, therefore, are not computationally efficient. On the other hand, every randomly generated UH and DRH vectors by the proposed method described later always satisfy the mass balance constraint. For a multivariate normal random vector subject to linear constraints, Borgman and Faucette (1993) recently developed an efficient method that converts the Gaussian linearly constrained simulation into the Gaussian conditional simulation which can be straightforwardly implemented.

In this paper, the algorithm of Gaussian linearly constrained simulation is described. For illustration, the simulation algorithm, in conjunction with the UH theory and routing techniques, are applied to evaluate the overtopping risk for a hypothetical flood detention reservoir at the downstream end of Tong-Tou watershed in Taiwan. Furthermore, elaborations are given to some potential extensions of the proposed simulation algorithm in the risk-based design and analysis of hydraulic slructures.

2 Uncertainty of UH

Yen et al. (1986) point out that the uncertainties in hydrology and hydraulics may be attributed to: (1) Natural uncertainties associated with the inherent randomness of natural processes; (2) Model uncertainty reflecting the inability of the simulation model or design procedure to represent precisely the system's true physical behavior; (3) Model parameter uncertainties resulting from inability to quantify accurately the model inputs and parameters; (4) Data uncertainties including measurement errors, inconsistency and non-homogeneity of data, and data handling and transcription errors; (5) Operational uncertainties including those associated with construction, manufacture, deterioration, maintenance, and other human factors that are not accounted for in the modeling or design procedure.

The UH theory assumes that the surface watershed is a linear, lumped, and time-invariant system which presents the model uncertainty because most watershed systems are non-linear, time-variant, and spatially distributed. Furthermore, measurement and data-processing errors in the ERH and DRH constitute data uncertainties. In the process of deriving a UH, these uncertainties will be transmitted to the resulting UH. Assessments of uncertainties associated with the derived UH have been made by using stochastic differential equation techniques (Sarino and Serrano, 1990; Hjelmfelt and Wang, 1994) for an instantaneous UH (IUH) based on Nash's model where the storage coefficient was considered as a normal random variable. Yang et al. (1992) showed that the two parameters, N and K, in Nash's IUH model in a watershed are negatively correlated, non-normal random variables. In the multiple-storm flamework, Zhao (1992)applied storm resampling techniques to quantify the uncertainty associated with a discrete UH of a specified duration from multiple complex storm events. Through an uncertainty analysis, the uncertainty features of a derived UH such as the mean and covariance matrix can be obtained.

3 Reliability analysis by monte-carlo simulation

Hydraulic or hydrologic routing is often required to evaluate the reliability of a hydraulic structure with the existing capacity. This makes the explicit quantification of risk difficult, if not impossible. Therefore, Monte-Carlo simulation is a viable tool for the task. Consider that the UH and DRH are multivariate random vectors and the given design ERH is deterministic. According to Eq. (1), the mean and covariance matrix associated with the DRH can be obtained, respectively, as:

$$\mathrm{E}(\mathbf{q}_{\mathrm{dsgn}}) = \mathbf{p}_{\mathrm{dsgn}}\,\mathrm{E}(\mathbf{u}) \tag{2}$$

$$\begin{aligned}\mathbf{C}(\mathbf{q}_{\mathrm{dsgn}} &= \mathrm{E}\left\{[\mathbf{q}_{\mathrm{dsgn}} - \mathrm{E}(\mathbf{q}_{\mathrm{dsgn}})]\,[\mathbf{q}_{\mathrm{dsgn}} - \mathrm{E}(\mathbf{q}_{\mathrm{dsgn}})]^{\mathrm{t}}\right\} \\ &= \mathbf{p}_{\mathrm{dsgn}}\mathrm{E}\left\{[\mathbf{u} - \mathrm{E}(\mathbf{u})]\,[\mathbf{u} - \mathrm{E}(\mathbf{u})]^{\mathrm{t}}\right\}\mathbf{p}_{\mathrm{dsgn}}^{\mathrm{t}} \\ &= \mathbf{p}_{\mathrm{dsgn}}\mathbf{C}(\mathbf{u})\,\mathbf{p}_{\mathrm{dsgn}}^{\mathrm{t}}\end{aligned} \tag{3}$$

in which $\mathrm{E}(\mathbf{u})$ and $\mathbf{C}(\mathbf{u})$ are, respectively, the mean vector and covariance matrix of the UH ordinates; $\mathrm{E}(\mathbf{q}_{\mathrm{dsgn}})$ and $\mathbf{C}\mathbf{q}_{\mathrm{dsgn}}$ are, respectively, the mean vector and the covariance matrix of design DRH ordinates; and the superscript 't' represents the transpose of a matrix or vector.

Once the mean and covariance matrix of the DRH corresponding to the design ERH are calculated, Monte-Carlo simulation can be used to generate random vectors of DRH based on an assumed probability distribution of the DRH or UH ordinates. The most commonly used multivariate distribution is the multivariate normal (Gaussian). If the UH vector follows a multivariate Gaussian distribution, then the DRH vector also has a multivariate Gaussian distribution because of the linear relationship between the UH and DRH vectors. Other multivariate distributions such as multivariate gamma and multivariate Pearson are discussed by Ronning (1977) and Parrish (1990), respectively. Recently, a practical approach for generating multivariate non-normal random variates with known marginal distributions has been proposed by Chang et al. (1994). The algorithm of implementing constrained non-normal multivariate simulation is yet to be developed and, therefore, this study will focus on multivariate normal distribution.

Two approaches can be used to generate random DRH vectors. The first approach is to generate random DRH vectors according to the mean vector and covariance matrix of $\mathbf{q}_{dsgn}$ as derived from Eqs. (2) and (3). The second approach is to generate random UH vectors based on the mean vector and covariance matrix of $\mathbf{u}$. Each of the generated UH vectors is then convolved with the design ERH by Eq.(1) to yield the corresponding design DRH. Although these two approaches give the same numerical solutions, a difference in computation efficiency between them should be mentioned here. If there is only one design ERH to consider in the design or analysis, there is no need to generate UH vectors and use them to convolve with the design ERH to obtain the design DRHs. Therefore, the first approach is more direct than the second approach when there is only one design ERH. On the other hand, if there are several design ERHs to consider, the second approach is recommended because the generated UHs can be stored and used at later time to convolve with different design ERHs by Eq. (1). If the first approach is used for several design ERHs, one has to generate a number of DRHs for each design ERH, which is computationally less efficient than the second approach.

However, one unique feature that must be observed in the Monte-Carlo simulation conducted herein. By the first approach, the generated DRHs must satisfy the mass balance constraint, namely, the water volume of each generated DRH must equal to that of the design ERH. When the second approach is used, each of the generated UHs must satisfy its definition, that is, the water volume of the generated UHs must equal to one inch (or cm) over the watershed. By either approach, one needs to obtain design DRHs, each of which satisfies the appropriate constraint.

Suppose a hydraulic structure such as a flood detention reservoir or levee for flood control purposes is located at the downstream end of the surface watershed. The output from the upstream watershed is the input to the downstream detention reservoir or levee. Therefore, the generated design DRHs, combined with the baseflow, are routed through the hydraulic structure among which some of them will cause the failure of the hydraulic structure. The fraction of simulations in which the failure of hydraulic structure occurs is the failure probability. Information such as this is important for the evaluation and modification of the hydraulic structure under consideration. From the Monte-Carlo simulation, other pertinent information about the failure characteristics can also be assessed.

Herein, the Gaussian linearly constrained simulation algorithm, in conjunction with the UH theory, are used for reliability analysis. Before the algorithm of Gaussian linearly constrained simulation for UH-based reliability analysis is derived, the Gaussian unconditional simulation and Gaussian conditional simulation will be presented due to the following two reasons: (1) the Gaussian linearly constrained simulation can be conducted under the framework of Gaussian conditional simulation, and (2) the Gaussian conditional simulation requires the use of the Gaussian unconditional simulation.

3.1 Gaussian unconditional simulation

Let $\mathbf{X}$ be a vector involving n multivariate normal random variables with the mean vector $\boldsymbol{\mu}_x$ and covariance matrix $\mathbf{C}_x$. The unconditional simulation (US) generates random $\mathbf{x}$'s based on the known mean vector $\boldsymbol{\mu}_x$ and covariance matrix $\mathbf{C}_x$. There are several efficient algorithms for generating multivariate Gaussian random vectors. The algorithm based on eigenvector-eigenvalue (spectral) decomposition is as follows:

1. Perform eigenvector-eigenvalue decomposition of $\mathbf{C}_x=\mathbf{V}_x\mathbf{L}_x\mathbf{V}_x^t$ in which $\mathbf{V}_x$ is an orthogonal eigenvectors matrix, and L is a diagonal matrix whose elements are the eigenvalues of $\mathbf{C}_x$.
2. Generate an independent normal random vector $\mathbf{z}$ having mean $\mathbf{0}$ and covariance matrix I, an identity matrix.
3. $\mathbf{x}^{(US)} = \mathbf{V}_x\ \mathbf{L}_x^{0.5}\ \mathbf{z} + \boldsymbol{\mu}_x$
4. Repeat (2)-(3) a large number of times to obtain many $\mathbf{x}$'s. The number of simulation depends on each individual model.

3.2 Gaussian conditional simulation

The Gaussian conditional simulation (CS) is to generate normal random vector $\mathbf{X}_2$ given $\mathbf{X}_1=\mathbf{x}_1$ where

$$\mathbf{X} = \begin{pmatrix} \mathbf{X}_1 \\ \mathbf{X}_2 \end{pmatrix} \tag{4}$$

and

$$\begin{pmatrix} \mathbf{X}_1 \\ \mathbf{X}_2 \end{pmatrix} \sim \mathrm{N}\left(\begin{bmatrix} \boldsymbol{\mu}_{x,1} \\ \boldsymbol{\mu}_{x,2} \end{bmatrix}, \begin{bmatrix} \mathbf{C}_{x,11} & \mathbf{C}_{x,12} \\ \mathbf{C}_{x,12}^t & \mathbf{C}_{x,22} \end{bmatrix} \right) \tag{5}$$

Steps (1)-(3) for the Gaussian conditional simulation are the same as those for the Gaussian unconditional simulation presented in Section 3.1. The following steps (4) and (5) are for the conditional simulation:

(4) Calculate

$$\mathbf{x}_2^{(CS)} = \mathbf{C}_{x,12}^t\mathbf{C}_{x,11}^{-1}\left(\mathbf{x}_1 - \mathbf{x}_1^{(US)}\right) + \mathbf{x}_2^{(US)} \tag{6}$$

(5) Repeat (2)-(4) a large number of times to obtain many conditional $\mathbf{x}_2$'s.

3.3 Gaussian linearly constrained simulation

Borgman and Faucette (1993) proposed an efficient procedure that converts the Gaussian linearly constrained simulation into the Gaussian conditional simulation. In the present problem context, only one simple constraint is involved. More specifically, the Gaussian linearly constrained simulation attempts to generate a J-element random vector $\mathbf{X}$ subject to a linear constraint that

$$\sum_{j=1}^{J} x_j = \mathbf{1}^t\mathbf{x} = \text{constant} \tag{7}$$

where $\mathbf{1}$ is a column vector of ones. To convert the Gaussian linearly constrained simulation into the Gaussian conditional simulation, one defines a new (J+1)-element random vector, $\mathbf{Y}$, as

$$\mathbf{Y} = \begin{pmatrix} Y_1 \\ \mathbf{Y}_2 \end{pmatrix} = \begin{pmatrix} \mathbf{1}^t\mathbf{x} \\ \mathbf{X} \end{pmatrix} = \mathbf{TX} \tag{8}$$

where Y_1 is a scalar, $\mathbf{Y}_2 = \mathbf{X}$, and

$$\mathbf{T} = \begin{pmatrix} 1 & 1 & \cdots & 1 & 1 \\ 1 & \mathbf{0} & \cdots & \mathbf{0} & \mathbf{0} \\ \mathbf{0} & 1 & \cdots & \mathbf{0} & \mathbf{0} \\ \cdot & \cdot & \cdot & \cdot & \mathbf{0} \\ \mathbf{0} & \mathbf{0} & \mathbf{0} & \mathbf{0} & 1 \end{pmatrix}_{(J+1)xJ} \tag{9}$$

Then, the mean and covariance matrix of $\mathbf{Y}$, respectively, are

$$\boldsymbol{\mu}_{\mathbf{Y}} = \mathbf{T}\boldsymbol{\mu}_{\mathbf{X}} \tag{10}$$

$$\mathbf{C}_{\mathbf{Y}} = \mathbf{T}\,\mathbf{C}_{\mathbf{X}}\mathbf{T}^t \tag{11}$$

Now, the Gaussian linearly constrained simulation of $\mathbf{X}$ can be converted into the conditional simulation of $\mathbf{Y}_2$, given $Y_1 = y_1 =$ constant, as

$$\mathbf{x} = \mathbf{y}_2^{(CS)} = \mathbf{C}_{y,12}^t\,\mathbf{C}_{y,11}^{-1}\left(y_1 - y_1^{(US)}\right) + \mathbf{y}_2^{(US)} \tag{12}$$

Then, the Gaussian conditional simulation algorithm can be used to generate a number of $\mathbf{x}$'s, each of which is subject to the linear constraint (Eq. (7)).

If the first approach is used to generate random design DRH vectors, then the Gaussian linearly constrained algorithm can be used by letting $\mathbf{x}$ = DRH and properly defining the constant in Eq. (7) such that the volume of water of each generated DRH is equal to that of the design ERH. If the second approach is used to generate random UHs, then the algorithm can be applied by letting $\mathbf{x}$ = UH and properly defining the constant in Eq. (7) such that the water volume of each generated UH is equal to one inch (or cm) over the watershed.

4 Application and discussions

For illustration, the Gaussian linearly constrained simulation presented above was applied to generate random UHs and DRHs for evaluating the overtopping probability of a hypothetical flood detention reservoir at the downstream end of Tong-Tou watershed (259.2 km^2) in Taiwan. The concern is given to typhoon storm events that could threat the safety of the dam. Recently, Zhao et al. (1995) applied five statistical validation methods to evaluate the predictability of UHs estimated by various least-squared-based methods in conjunction with storm-stacking, storm-combining, storm-scaling, and single-storm averaging methods when data from several storms are available for estimating the UH. The least-squares-based methods considered include the ordinary least squares (OLS), the ridge least squares with the mimmization of the mean squared error of UH (RDG/UH), and the ridge least squares with the mimmization of the mean squared error of DRH (RDG/DRH). The storm-stacking method is the conventional multiple-storm analysis. The storm-combining method is to directly add the DRH ordinates of all storms and ERH ordinates of all storms, respectively, to form a single DRH and ERH for a combined storm. The storm-scaling is to scale all storms so that all storms have the same amount of effective rainfall

depth of one unit. The storm-scaling method is achieved through dividing the ERH and DRH ordinates by the ER amount for each storm.

The most important finding from the validation study is that the storm-stacking with storm-scaling gives the smallest prediction errors. Applications of the five validation methods to Tong-Tou watershed indicate the prediction error by the RDG/DRH is smaller than that by the RDG/UH. Three out of five validation methods for Tong-Tou watershed also show that the prediction error by the RDG/DRH is smaller than that by the OLS. Therefore, the storm-stacking along with storm-scaling and the RDG/DRH is used herein to derive the representative UH. Rainfall-runoff data from seven typhoon events were used to estimate the UH ordinates for the watershed. The duration of the derived UH is 3 hours.

For illustration, the adopted design ERH, as shown in Figure 1, was made of the largest ordinates of the observed ERHs at each of the 3-hour time intervals from the seven storm events used in UH derivation. The baseflow for Tong-Tou is 2.832 cms which contribute little to the occurrence of overtopping. The height of the hypothetical detention reservoir is 9.144 meters having a controlled outlet allowing a maximum constant discharge of 849.5 cms without causing the detention reservoir to overtop. The elevation-storage curve and elevation-outflow curve for the hypothetical detention reservoir are shown in Figures 2 and 3, respectively. In this example application, the design ERH, for simplicity, is considered deterministic.

To apply the Gaussian linearly constrained Monte-Carlo simulation for assessing the overtopping probability, the statistical characteristics of UH vector such as its mean and covariance matrix must be known or assessed. Based on the concept of bootstrap technique (Efron, 1982; Efron and Tibshirani, 1986), Zhao (1992) developed a storm resampling technique to quantify uncertainty features associated with the UH by the multiple-storm method. The basic idea of the bootstrap technique is to extract more information from one observed random sample to better understand the population (or the statistics associated with the population) by resampling this observed random sample a large number of times. In the storm resampling scheme, the observed storm events are considered as random samples. A large number of samples can be obtained by resampling, *with* replacement, the original observed storms a large number of times. Each sample is called a bootstrap storm sample from which a multiple-storm unit hydrograph is derived. The aforementioned bootstrap is called unbalanced bootstrap. The balanced bootstrap resampling only reuses each of the sample observations exactly equally often.

Both balanced and unbalanced bootstrap techniques were used for purpose of comparison. One thousand (1000) bootstrapped multiple-storm UHs based on the seven typhoon storm events occurred in Tong-tou watershed were obtained. The mean and standard deviation vectors of the multiple-storm UH vector from the ridge least squared method are shown in Table 1. As can be seen that there is little difference in the mean value for each UH ordinate between the unbalanced and balanced bootstrap methods. However, the standard deviation for most UH ordinates by the balanced bootstrap is slightly higher than that by the unbalanced bootstrap, indicating that there exist slightly larger uncertainties in the UH ordinates by the balanced bootstrapping. The correlation matrix associated with the UH ordinates by the unbalanced and balanced bootstrap techniques are shown in Tables 2(a) and 2(b). No significant difference in the correlation matrices between both methods can be observed.

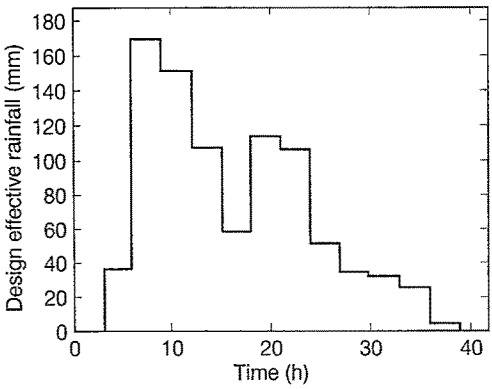

Figure 1. Design effective rainfall hyteograph in hypothetical example.

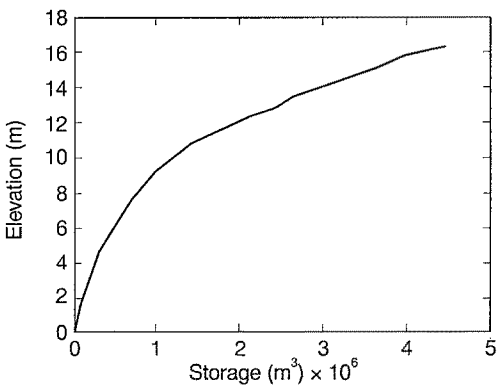

Figure 2. Elevation-storage curve for the hypothetical detention reservoir.

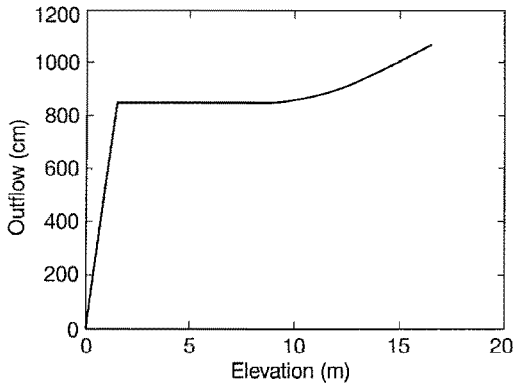

Figure 3. Elevation-outflow curve for the hypothetical detention reservoir.

Table 1. Means and Standard Deviations of the Multiple-Storm UI-Is by Ridge Least Squared Method with Scaling Using Balanced and Unbalanced Bootstrap Techniques

	Unbalanced bootstrap		Balanced bootstrap	
	Mean	Std	Mean	Std
UH(1)	7.147e+00	9.502e-01	7.154e+00	9.573e-01
UH(2)	5.902e+00	4.959e-01	5.914e+00	5.291e-01
UH(3)	2.586e+00	3.035e-01	2.571e+00	3.114e-01
UH(4)	1.378e+00	3.127e-01	1.370e+00	3.200e-01
UH(5)	1.483e+00	3.116e-01	1.495e+00	3.206e-01
UH(6)	1.385e+00	1.832e-01	1.389e+00	1.848e-01
UH(7)	8.768e-01	9.410e-02	8.707e-01	1.033e-01
UH(8)	8.228e-01	9.713e-02	8.175e-01	1.019e-01
UH(9)	6.107e-01	5.581e-02	6.092e-01	5.855e-02
UH(10)	5.080e-01	5.143e-02	5.061e-01	5.592e-02
UH(11)	3.379e-01	6.209e-02	3.366e-01	6.669e-02
UH(12)	3.335e-01	3.727e-02	3.349e-01	4.102e-02
UH(13)	2.301e-01	3.862e-02	2.290e-01	4.184e-02
UH(14)	1.997e-01	2.599e-02	1.996e-01	3.029e-02
UH(15)	1.598e-01	1.837e-02	1.589e-01	1.994e-02
UH(16)	1.282e-01	1.307e-02	1.280e-01	1.436e-02
UH(17)	8.708e-02	1.161e-02	8.713e-02	1.488e-02
UH(18)	6.301e-02	1.229e-02	6.263e-02	1.466e-02
UH(19)	3.139e-02	1.222e-02	3.095e-02	1.287e-02
UH(20)	1.961e-03	5.593e-03	1.920e-03	5.446e-03

Table 2. Correlation Matrices of 3-Hr UH Ordinates for Tong-tou Watershed from Unbalanced and Balanced Bootstrap Techniques

(a) From Unbalanced Boostrapping

	u(1)	u(2)	u(3)	u(4)	u(5)	u(6)	u(7)	u(8)	u(9)	u(10)	u(11)	u(1 2)	u(13)	u(14)	u(15)	u(16)	u(17)	u(18)	u(19)	u(20)
u(1)	1.000																			
u(2)	-0.274	1.000																		
u(3)	-0.774	-0.002	1.000																	
u(4)	-0.094	-0.030	0.009	1.000																
u(5)	-0.577	-0.093	-0.292	-0.208	1.000															
u(6)	0.006	-0.193	-0.147	0.412	0.092	1.000														
u(7)	-0.010	0.276	0.333	0.054	-0.046	0.242	1.000													
u(8)	-0.217	0.228	0.313	-0.236	-0.005	0.099	0.343	1.000												
u(9)	-0.237	0.074	0.185	0.131	0.127	0.446	0.227	0.321	1.000											
u(10)	-0.236	0.012	0.334	-0.295	-0.038	-0.299	0.342	0.536	-0.257	1.000										
u(11)	0.192	-0.828	0.064	-0.176	0.097	-0.113	0.301	-0.435	-0.276	0.153	1.000									
u(12)	-0.465	0.067	0.082	0.479	0.440	0.402	0.017	-0.220	-0.022	0.047	0.005	1.000								
u(13)	-0.483	0.374	0.573	0.434	0.330	0.315	0.584	-0.053	0.195	0.101	0.388	0.500	1.000							
u(14)	-0.501	0.034	0.297	0.564	0.323	0.592	0.385	0.099	0.161	0.146	-0.035	0.794	0.719	1.000						
u(15)	-0.206	-0.570	0.372	0.251	0.340	0.325	0.694	-0.077	0.182	-0.004	0.548	0.240	0.846	0.518	1.000					
u(16)	-0.288	-0.036	0.073	0.470	0.311	0.625	0.360	0.230	0.273	0.108	-0.133	0.629	0.539	0.884	0.462	1.000				
u(17)	-0.130	-0.270	0.134	0.063	0.268	0.227	0.398	-0.061	0.264	0.015	0.305	0.120	0.528	0.316	0.617	0.396	1.000			
u(18)	-0.299	0.045	0.109	0.399	0.214	0.043	-0.037	-0.194	-0.086	0.001	0.021	0.578	0.294	0.415	0.121	0.304	-0.353	1.000		
u(19)	-0.240	-0.471	0.276	0.213	0.269	0.211	0.131	-0.325	0.117	-0.146	0.465	0.363	0.560	0.352	0.460	0.236	0.203	0.193	1.000	
u(20)	-0.067	-0.194	-0.078	0.426	0.040	0.218	-0.026	-0.396	0.103	-0.299	0.178	0.390	0.352	0.340	0.304	0.303	0.291	0.286	0.349	1.000

(b) From Balanced Boostrapping

	u(1)	u(2)	u(3)	u(4)	u(5)	u(6)	u(7)	u(8)	u(9)	u(10)	u(11)	u(1 2)	u(13)	u(14)	u(15)	u(16)	u(17)	u(18)	u(19)	u(20)
u(1)	1.000																			
u(2)	-0.306	1.000																		
u(3)	-0.737	-0.029	1.000																	
u(4)	-0.102	0.056	-0.034	1.000																
u(5)	-0.536	-0.087	0.229	-0.208	1.000															
u(6)	-0.026	-0.221	-0.102	0.404	0.177	1.000														
u(7)	-0.173	-0.216	0.374	0.101	-0.064	0.171	1.000													
u(8)	-0.275	0.230	0.370	-0.216	-0.006	0.098	0.284	1.000												
u(9)	-0.267	0.068	0.229	0.060	0.130	0.343	0.179	0.331	1.000											
u(10)	-0.260	0.060	0.349	-0.207	-0.089	-0.312	0.324	0.537	-0.102	1.000										
u(11)	0.230	-0.830	0.105	-0.183	0.049	-0.103	0.256	-0.408	-0.176	0.135	1.000									
u(12)	-0.461	0.136	0.010	0.512	0.411	0.400	0.060	-0.218	-0.801	0.047	-0.086	1.000								
u(13)	-0.431	-0.381	0.511	0.405	0.322	0.381	0.578	-0.067	0.054	-0.006	0.338	0.460	1.000							
u(14)	-0.472	-0.019	0.218	0.533	0.354	0.608	0.329	0.053	-0.003	0.020	-0.119	0.788	0.713	1.000						
u(15)	-0.185	-0.571	0.376	0.228	0.319	0.335	0.691	-0.834	0.122	-0.061	0.518	0.171	0.840	0.458	1.000					
u(16)	-0.315	0.014	0.085	0.464	0.260	0.574	0.253	0.274	0.270	0.233	-0.136	0.580	0.371	0.712	0.304	1.000				
u(17)	-0.078	-0.189	0.172	-0.051	0.120	0.016	0.342	0.060	0.401	0.206	0.308	-0.117	0.184	-0.808	0.399	0.299	1.000			
u(18)	-0.296	0.074	0.074	0.432	0.153	0.108	-0.066	-0.175	-0.006	0.070	0.019	0.587	0.213	0.376	0.033	0.364	-0.368	1.000		
u(19)	-0.204	-0.501	0.316	0.231	0.165	0.170	0.203	-0.294	0.118	-0.109	0.509	0.276	0.516	0.282	0.458	0.177	0.121	0.212	1.000	
u(20)	-0.056	-0.200	-0.067	0.381	0.023	0.191	-0.035	-0.389	0.109	-0.275	0.194	0.324	0.294	0.256	0.253	0.230	0.201	0.234	0.338	1.000

To evaluate the probability of overtopping, one can directly simulate a large number of DRHs by using the Gaussian linearly constrained simulation after the mean vector and covariance matrix of the DRH are computed by Eqs. (2) and (3). In this example application, 2000 simulation runs were made to generate DRHs by the Gaussian linearly constrained simulation. Then, the baseflow is added to the generated DRHs to form the total runoff hydrographs which serve as the inflow hydrographs to the hypothetical detention reservoir. The level pool routing was performed to route these inflow hydrographs through the detention reservoir (Chow et al., 1988).

Figures 4 and 5, respectively, show 20 simulated 3-hr UHs and the corresponding design DRHs. For the specified detention reservoir height, some of the simulated inflow hydrographs may overtop the detention reservoir, resulting in performance failure of the detention reservoir. The probability of overtopping for the detention reservoir is estimated by the fraction of simulations in the total simulation runs that overtopping event occurs. One can also estimate the statistical features of overtopping characteristics such as overflow duration, overflow peak, and overflow volume.

Table 3 presents the estimated overtopping risks for the hypothetical detention reservoir by the unbalanced and balanced bootstrap techniques. One can observe that there is no significant difference between these two techniques. This could be attributed to the similarities of the statistical properties of UHs estimated by the balanced and unbalanced bootstrap techniques as shown in Table 1. However, the effect of difference in standard deviations between the two bootstrap techniques is revealed in the calculated overtopping risk as shown in Table 3. As expected, the overtopping risk associated with the balanced bootstrap procedure is somewhat higher than that of the unbalanced procedure due to a slightly larger standard deviation in the UH ordinates by the balanced bootstrapping.

Table 4 summarizes the statistics of overflow duration, peak, and volume from the simulation. Again, there is no significant difference in the mean values of overflow duration between the two bootstrap procedures. It can be seen that the skewness of overtopping duration, peak and volume are all positive and the values of skewness for duration are smaller than those for peak and volume. Figure 6 shows the histograms of overtopping duration, peak, and volume from the simulation. Table 5 presents the correlation coefficients of overflow characteristics such as overflow duration, peak, and volume. All correlation coefficients are positive, which is consistent with the expected general behaviors. It can be observed that the correlation between the overflow peak and overflow volume is the strongest.

The information in Table 3-5 is useful in risk-based hydraulic design for detention reservoirs. For each possible reservoir sizing strategy, one can compute the risk as in Table 3 and then select the optimal strategy based on the criteria of high efficiency, low cost, and acceptable overtopping risk. Then the possible damage due to overtopping is assessed by using the values of overtopping duration, overtopping peak, and overtopping volume. Because the overtopping duration, overtopping peak, and overtopping volume are random variables whose statistics are obtained as in Table 4-5, the damage is also a random variable. One then can compute the statistics of the damage, which includes the expected value, standard deviation, confidence intervals, and so on. For a more comprehensive risk-based hydrologic and hydraulic design, one can select an optimal detention reservoir sizing such that a weighted sum of the expected value and variance of overtopping damage is minimized.

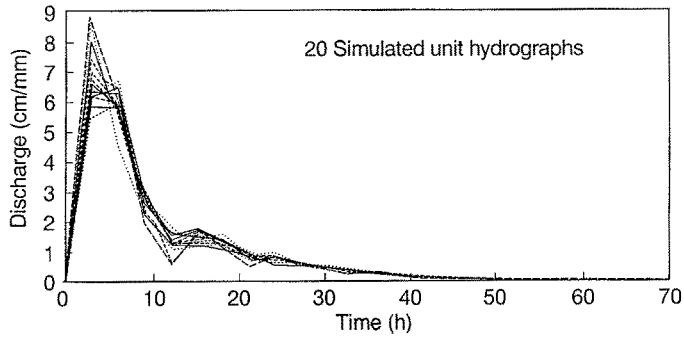

Figure 4. Sample simulated unit hydrographs.

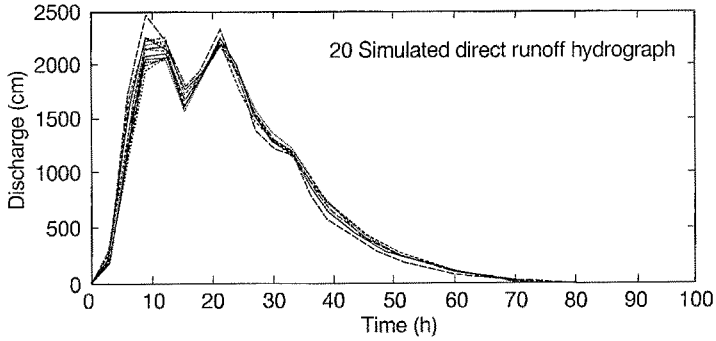

Figure 5. Sample simulated direct runoff hydrographs.

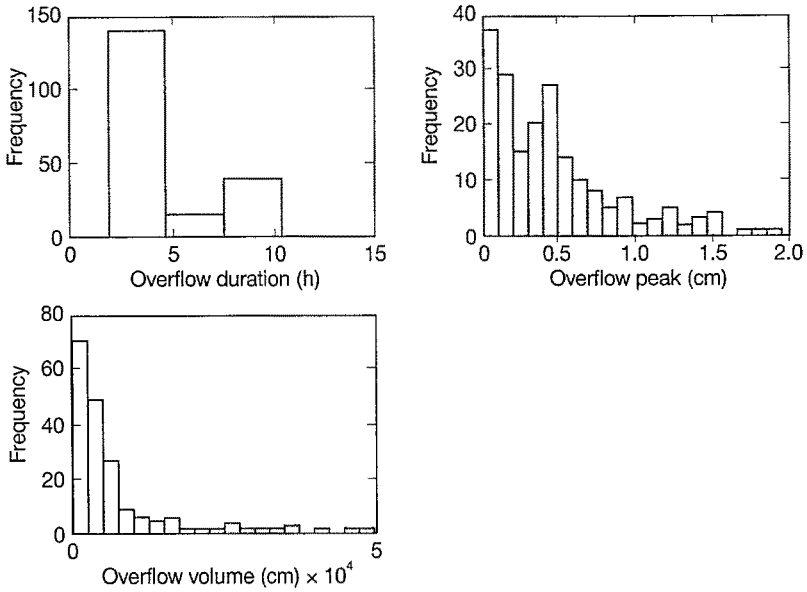

Figure 6. Histograms of simulated overflow duration, overflow volume, and overflow peak.

Table 3. Risk of Detention Reservoir Overflow Based on the Simulation Results by Various Methods.

	Storm-stacking with scaling
Unbalanced bootstrap	0.0810
Balanced bootstrap	0.0970

Table 4. Summary Statistics of Overflow Characteristics Based on the Mean and Covariance Matrix of UH Derived from Various Methods for the Tong-Tou Watershed.

	Unbalanced bootstrap			Balanced bootstrap		
	Duration (hours)	Peak (cms)	Volume (cubic meter)	Duration (hours)	Peak (cms)	Volume (cubic meter)
Mean	4.500e+00	4.444e-01	6.686e+03	4.438e+00	4.591e-01	7.114e+03
STD	2.439e+00	3.801e-01	8.163e+03	2.427e+00	4.129e-01	9.318e+03
CV	1.844e+00	1.169e+00	8.191e-01	1.827e+00	1.111e+00	7.634e-01
Skewness	1.157e+00	1.165e+00	2.093e+00	1.222e+00	1.341e+00	2.270e+00

Table 5. Correlation Coefficient Between the Simulated Overflow Duration, Peak, and Volume from Various Methods for the Tong-Tou Watershed.

(a) By Unbalanced Bootstrap

	Overflow Duration	Overflow Peak
Overflow Peak	0.8809	
Overflow Volume	0.8555	0.9666

(b) By Balanced Bootstrap

	Overflow Duration	Overflow Peak
Overflow Peak	0.8581	
Overflow Volume	0.8362	0.9672

5 Summary and conclusions

Hydraulic structures are always placed in stochastic envirouments and their abilities to serve the intended functions generally cannot be ensured. Under such circumstances, reliability is an important issue in hydraulic structure system designs and performance evaluations. Unit hydrograph is a widely used rainfall-runoff model for deriving discharge hydrograph used in design and performance evaluation of hydraulic structures. Due to the existence of various uncertainties, the derived unit hydrograph unavoidably is subject to uncertainty which, in turn, results in uncertainty in the design discharge hydrograph.

In this paper, reliability analysis based on the Gaussian linearly constrained simulation in conjunction with UH theory and a routing method was presented and applied to the evaluate the overtopping probability of a hypothetical detention reservoir. The linearly constrained simulation is required because of the physical relationship among the unit hydrograph ordinates and direct runoff hydrograph ordinates. It should be kept in mind that the Gaussian linearly constrained simulation applied in this paper assumes that unit hydrograph or direct runoff hydrograph ordinates are multivariate normal variables and the variables are linearly related. Further development is needed for multivariate hydrological simulations in which variables are non-normal and nonlinearly related. The proposed methodology can be applied to other hydraulic structures for risk-based design and analysis.

The present paper considers only the uncertainty of the UH in the reliability analysis of hydraulic structures. The design storm hyetograph, which in reality is uncertain, is treated as known and deterministic. Therefore, the overtopping risk presented in Table 3 should be regarded as conditional upon the specified design rainfall hyetograph. To incorporate uncertainty in the design storm hyetograph, analysis is required with regard to the rainfall depth-duration-frequency relationship and the temporal distribution of storm. Once the uncertainty features of design storm hyetograph are available, the constrained simulation framework presented in the paper can be applied.

Acknowledgments

The study was sponsored in part by the Agricultural Council of the Executive Yuan, Taiwan, Republic of China, and the Wyoming Water Resources Center. Gratitude is extended to Mr. Wen-Jung Hu of the Agricultural Council for his support and to Ms. Yue-Chuan Huang of the Provincial Water Conservancy Bureau for her supply of rainfall-runoff data. The authors are also very grateful to the editor and the anonymous reviewers for their constructive comments.

References

Ang. A. H-S.; Tang, W. H. Probability Concepts in Engineering Planning and Design, Vol. II: Design, Risk, and Reliability, New York, N.Y.: John Wiley and Sons, Inc. 562 pp

Borgman, L.E. 1990: Irregular ocean waves: kinematics and forces. Ocean Engineering Science. Ed. by Mehaute, B.L. and Hanes, D.M., New York, N.Y.: John Wiley and Sons, Inc.

Borgman, L.E.; Faucette, R.C. 1993: Frequency-domain simulation and stochastic interpolation of random vectors in multidimensional space. Computational Stochastic Mechanics. Ed. by H-D Cheng and C.Y. Yang

Chang, C.H.; Tung, Y.K.; Yang, J.C. 1994: Monte carlo simulation for correlated variables with marginal distributions. J. of Hydraulic Engr., ASCE, 120(2), 313-331

Chow, V.T.; Maidment, D.R.; Mays, L.W. 1988: Applied Hydrology. New York: McGraw-Hill Book Company. 572 pp

Efron, B. 1982: The Jackknife, the Bootstrap and Other Resampling Plans, CBMS 38, SIAM

Efron, B.; Tibshirani, R. 1986: Bootstrap methods for standard errors, confidence intervals, and other measures of statistical accuracy. Statistical Science, 1(1), 54-77

Fiering, M.B.; Jackson, B.B. 1971: Synthetic Streamflows, Washington, D.C.: American Geophysical Union

Freudenthal, A.M. 1947: The safety of structures. Transactions, ASCE, 112, 125-180

Freudenthal, A.M. 1956: The safety and the probability of structural failure. Transactions, ASCE, 121, 1337-1397

Hjelmfelt, A.; Wang, M. 1994: General stochastic unit hydrograph. J. of Irrigation and Drainage Engineering, ASCE, 120(1), 138-148

Hufschmidt, M.M.; Fiering, M.B. 1966: Simulation Techniques for Design of Water-Resource Systems. Cambridge, Massachusetts: Harvard University Press.

Mizumura, K.; Ouazar, D. 1992: Stochastic characteristics of open channel flow. Stochastic Hydraulics '92, edited by J.T. Kuo and G.F. Lin. Proc. of 6th IAHR International Symposium on Stochastic Hydraulics. Department of Civil Engineering, National Taiwan University, Taipei, Taiwan, 417-423

Nguyen, V.U.; Chowdhury, R.N. 1985: Simulation for risk analysis with correlated variables. Geotechnique, 35(1), 47-58

Parrish, R. S. 1990: Generating random deviates from multivariate Pearson distributions. Computational statistics and Data analysis, 9, 283-295

Ronning, G. 1977: A simple scheme for generating multivariate gamma distributions with nonnegative. Technometfics, 19(2), 179-183

Rubinstein, R. Y. 1981: Simulation and the Monte Carlo Method, New York: John Wiley and Sons, Inc. 278 pp

Sarino; Serrano, S.E. 1990: Development of the instantaneous unit hydrograph using stochastic differential equations. J. of Stochastic Hydrology and Hydraulics, 4, 151-160

Shinozuka, M. 1964: Probability of structural failure under random loading. J. of EMD, ASCE, 90(5), 147-170

Shinozuka, M. 1981: Stochastic characterization of loads and load Combinations, In: Structural Safety and Reliability, Ed. by Moan, T. and Shinozuka, M., New York, N.Y.: Elsevier Scientific Publishers

Shinozuka, M. 1989: Developments in structural reliability. In: Structural Safety and Reliability, Ed. by Ang, A. H-S., Shinozuka, M., and Schueller, New York, N.Y.: ASCE

von Neumann, J. 1951: Various techniques used in connection with random digits. U.S. Nat. Bur. Stand. Appl. Math. Ser., 12, 36,38

Yang, J.C.; Tung, Y.K.; Tang, S.Y.; Zhao, B. 1992: Uncertainty analysis of hydrologic model and its implications on reliability of hydraulic structures (I). Report, Agricultural Council, Executive Yuan, Taiwan, Republic of China. 240 pp

Yen, B.C.; Tung, Y.K. 1993: Reliability and Uncertainties in Hydraulic Designs, ASCE, New York, NY

Yen, B.C.; Cheng, S.T.; Melching, C.S. 1986: First Order Reliability Analysis. In: Stochastic and Risk Analysis in Hydraulic Engineering, B.C. Yen, ed., Littleton, CO: Water Resources Publications

Zhao, B. 1992: Determination of a unit hydrograph and its uncertainty applied to reliability analysis of hydraulic structures. M.S. Thesis, Department of Statistics, University of Wyoming, 352 pp

Zhao, B.; Tung, Y.K.; Yeh, K.C.; Yang, J.C. 1995: Statistical validation methods: Application to unit hydrographs. J. of Hydraulic Engineering, ASCE, 121(8), 618-625